applied sciences

MDPI

Article

Activation Analyses of Disposal Options for Irradiated $Be_{12}Ti$

Pavel Pereslavtsev [1,*], Pierre Cortes [2] and Joelle Elbez-Uzan [2]

[1] Karlsruhe Institute of Technology (KIT), Hermann-von-Helmholtz-Platz 1, Eggenstein-Leopoldshafen, 76344 Karlsruhe, Germany
[2] EUROFUSION Programme Management Unit, Fusion Technology Department—DEMO Central Team, Boltzmannstrasse 2, 85748 Garching, Germany; pierre.cortes@euro-fusion.org (P.C.); joelle.elbez-uzan@euro-fusion.org (J.E.-U.)
* Correspondence: pavel.pereslavtsev@kit.edu

Abstract: The activity and disposal options for irradiated $Be_{12}Ti$ were assessed for the HCPB DEMO blankets making use of a code system that enables performing 3D activation calculations by linking the Monte Carlo transport code MCNP and the fusion inventory code FISPACT through an appropriate interface. The dedicated full-scale geometry MCNP model of the 11.25 degree HCPB DEMO torus was adapted to the requirements for the coupled 3D neutron transport and activation calculations. Special attention was paid to the use in the activation calculations of the commercial materials containing technological impurities. This has a crucial effect on the results and the impurities must be accounted for in any nuclear safety analyses. The short-term activity is formed by the radionuclides produced through the activation of Be and Ti nuclei and the long-term activity is formed by the products of the neutron irradiation taking place on the impurities. A prerequisite for the disposal or the recycling of the irradiated $Be_{12}Ti$ is its deep detritiation; otherwise, the very high-tritium activity would fully prevent any attempt for its treatment. The most preferable is the use of the $Be_{12}Ti$ with the composition including less material impurities, especially uranium. There could be the option to dispose the $Be_{12}Ti$ intermediate-level wastes in the French repository after 1 year of cooling, assuming the detailed control of the impurities that fulfil the French authority requirements. The USA near-ground repositories could be an alternative to the European sites. The recycling of the irradiated $Be_{12}Ti$ must first be elaborated and approved to ensure its treatment in a safe and efficient way. The remote handling technique must be developed for the re-fabrication of the $Be_{12}Ti$ blocks.

Keywords: DEMO; neutron multiplier; $Be_{12}Ti$; neutronics; activation; disposal

Citation: Pereslavtsev, P.; Cortes, P.; Elbez-Uzan, J. Activation Analyses of Disposal Options for Irradiated $Be_{12}Ti$. *Appl. Sci.* **2023**, *13*, 7534. https://doi.org/10.3390/app13137534

Academic Editor: Francesco Caridi

Received: 30 May 2023
Revised: 20 June 2023
Accepted: 20 June 2023
Published: 26 June 2023

1. Introduction

The development of a conceptual design for a demonstration fusion power plant (DEMO) has the highest priority in the EUROfusion Fusion Technology Department programme [1]. Two different concepts are now in progress to be implemented as a driver blanket for the upcoming DEMO fusion reactor: WCLL (Water Cooled Lithium Lead) [2] and HCPB (Helium Cooled Pebble Bed) [3]. Because of different reactor technologies and materials utilized, these two concepts have their own *cons* and *pros* affecting R&D activity. Pressurized water (155 bar) assumed in the cooling system of the WCLL DEMO even in spite of a complex chemistry seems to have some advantages compared to He gas coolant: the PWR-like technology is cheap, well established and robust. Liquid lead used as a neutron multiplier is widespread and not expensive. Weak points in the WCLL blanket concept are a corrosion between PbLi eutectic and steel structure, a tritium permeation from PbLi through steel walls in the water coolant and a very sophisticated tritium extraction technology. A solid breeder used in the HCPB blanket provides an efficient tritium generation and its extraction from the helium purge gas. The main drawback of the HCPB blanket technology is the very high capital expenses of this DEMO concept.

The cost factor is extremely important for public acceptance of the fusion facility and the fusion energy. The main disadvantages of the $Be_{12}Ti$ neutron multiplier utilized in the HCPB breeder blanket are costs due to limited natural resources [4]. The price of raw beryllium increases continually with an annual rate of ~2.5%/year and it is estimated currently to be ~610 ÷ 650 USD/kg [4,5]. A conservative reasoning of the future price for the $Be_{12}Ti$ industrial production for the DEMO needs could be estimated to be at least 1000 ÷ 2000 USD/kg in 30 years depending on the beryllium market evolution. Namely, the restricted Be resources are the reasons for the initiated research activity to find a reasonable solution for a possible Be recycling or, in the worst case, to define conditions for a possible disposal of the irradiated $Be_{12}Ti$. A total load of the $Be_{12}Ti$ in the HCPB demo was estimated to be ~600 tons that corresponds to ~418 tons of Be [6]. In spite of the fact that the world's identified resources of beryllium have been estimated to be more than 100,000 tons, the total world Be production does not exceed ~260 tons [5]. It is highly probable that the total Be amount required for the production of the $Be_{12}Ti$ blocks for the HCPB breeder blankets will be provided from different global sources. Each Be ore possesses a specific chemical composition with various chemical element contents. As a result, the chemical composition of the Be (including impurities) used for the future HCPB breeder blankets cannot be defined exactly but it can be approximately assessed to make use of the available information for different Be ores.

An accumulation of radioactive nuclides in the $Be_{12}Ti$ is inherent in the process accompanying its utilization in the HCPB DEMO blanket due to intensive neutron irradiation. Depending on the initial chemical composition of the $Be_{12}Ti$, its final inventory can differ significantly, affecting its treatment and processing strategy. This report presents an assessment of $Be_{12}Ti$ activation in the current DEMO baseline model with the fully heterogeneous HCPB blanket concept reflecting the latest consolidated design and possible disposal options as well as outlines eventual recycling options.

2. $Be_{12}Ti$ Neutron Multiplier

2.1. Beryllium Resources

Beryllium is currently produced from two minerals: bertrandite ($Be_4Si2O_7(OH)_2$) and beryl ($Be_3Al_2Si_6O_{18}$) [5]. Bertrandite, which contains about 15 wt% beryllium, is the principal beryllium mineral mined in the United States. Beryl, which can contain up to 5 weight percent beryllium, is the main beryllium mineral mined in the rest of the world. Beryl ore typically contains from 2 to 4 weight percent beryllium. Countries with active industrial beryl mining operations include Brazil, China, Madagascar, Mozambique, Nigeria, Portugal, Rwanda and Uganda [5].

The United States, Kazakhstan and China are the only countries known to process beryllium ores and concentrates into beryllium products [7]. Materion Corporation, Parkland Blvd., USA is the only producer of beryllium ore in the United States. The JSC Ulba Metallurgical Plant of Kazakhstan produces beryllium hydroxide from stockpiled concentrate previously extracted from the Ermakovskoe beryllium deposit in Russia [7]. The concentrate stockpile total accumulated by 1992; it was estimated that the Ulba Metallurgical Plant produced about 90 tons of beryllium in 2015 contained in beryllium–copper alloys, beryllium oxide ceramics, and beryllium metal. China's Shuikoushan Non-Ferrous Metals Group Co., Ltd. mines beryllium ores to produce beryllium products in various forms at its refinery in Songbai, Hunan Province. The plant has an estimated production capacity of 150 metric tons per year of beryllium oxide (36 weight percent beryllium. The main beryllium world suppliers are listed in Table 1. In fact, the Materion (170 tons/year) and Ulba Plant (90 tons/year) are the major potential Be suppliers for the HCPB DEMO blankets.

Table 1. World mine Be production and reserves [5].

Country	Mine Production
USA	180
Brazil	3
China	70
Madagascar	1
Mozambique	13
Nigeria	1
Rwanda	1
Uganda	7
World total (rounded)	**280**

The world annual Be production presented in Table 1 is significantly below the total needs for the future HCPB DEMO. Because of its chemical properties, beryllium metal is required in many industrial applications. A wide variety of products made from beryllium are used in aerospace, computer, defense, medical, nuclear and telecommunications applications. In the USA, a high-purity beryllium metal is classified as a strategic and critical material because of its vital importance for national security [7]. Therefore, it is very unlikely that the beryllium demands for the HCPB DEMO exceeding its annual world production can be covered without a long-term buying strategy. The appearance of such an important consumer as the DEMO on the global market could very likely be a driving force for the Be price increase. Hence the economical factor has to be accounted for when developing a strategy for the beryllium handling within the EUROfusion DEMO project.

2.2. Beryllium Chemical Composition

The impurities content in the original raw Be is the crucial issue for the future strategy of the industrial handling of the irradiated beryllium [6]. The concentration of various impurities significantly affects the results of the berillium activity accumulated during the irradiation phase. For the purposes of this work, the following assumption was made: the majority of the beryllium for the HCPB blanket manufacture will very likely come from the main suppliers, namely, from the Ulba (stands for JSC Ulba Metallurgical Plant of Kazakhstan) and/or from the Materion (which stands for Materion Corporation, Parkland Blvd., USA). The $Be_{12}Ti$ will be produced utilizing beryllium: (1) from one of them, (2) separately from each of them or (3) from the mixture of them. Listed in Table 2 are the chemical compositions of berillium from the Ulba, PTB-56 [8] and nuclear grade S-65 beryllium for the International Thermonuclear Experimental Reactor (ITER) from the Materion [9]. A chemical composition of Ti (RP-Ti grade OM-1, Polema [8]) is given in Table 3.

Table 2. Chemical compositions (wt%) of the Be from Ulba and Materion.

Element	Ulba	Materion
Be	*balance*	*balance*
BeO	-	0.9000
C	0.0500	0.0900
Fe	0.1000	0.0800
Al	0.0200	0.0500
Si	0.0300	0.0450

Table 2. *Cont.*

Element	Ulba	Materion
Mg	0.0200	0.0100
Zn	-	0.0050
Cr	0.0200	0.0100
Ni	0.0200	0.0250
Cu	0.0100	0.0250
Ti	-	0.0250
Zr	-	0.0050
U	0.0002	0.0150
Mn	0.0100	0.0050
Ag	-	0.0050
Co	-	0.0050
Pb	0.0500	0.0050
Ca	0.0050	0.0050
Mo	-	0.0050
O	0.8000	-
F	0.0010	-
Other	-	0.0400

Table 3. Chemical composition of Ti.

Element	Ti	Si	Fe	Ni	C	N	H
wt%	*balance*	0.10	0.20	0.20	0.05	0.08	0.35

An essential difference of the Be compositions presented in Table 2 is the uranium content. The presence of the uranium impurity is not of concern in case of the Be for the industrial applications without neutron irradiation. A quite different context is in nuclear facilities with the neutron irradiation where the utilization of beryllium will inherently result in an accumulation of α-radioactive and toxic transuranic isotopes of U, Pu, Am and Cm [10]. This will dramatically change the handling strategy of the irradiated $Be_{12}Ti$ and its clearance according to IAEA recommendations [11] and could be unavoidable. Other impurities are also of high interest due to (a) the potential environmental risk and (b) the potential danger during a treatment.

2.3. $Be_{12}Ti$ Chemical Composition

Eventually, Be for HCPB DEMO needs could originate not only from the main suppliers such as Materion and Ulba but rather from several other suppliers including minor providers. It is difficult nowadays to create an outline of the manufacturing strategy for $Be_{12}Ti$ blocks. Generally, they can be produced either in different factories supplied by the domestic ores or Be could also be transported from various sources to collect and mix it in one place for its unified treatment and production. The latter option looks more feasible because it does not suppose a know-how transfer of the newly developed technology of the $Be_{12}Ti$ blocks production [8]. Independently of the strategy, HCPB DEMO breeder blankets will be very likely filled with $Be_{12}Ti$ blocks having slightly different material compositions. To account for the spread in the impurities content, three sets of the $Be_{12}Ti$ chemical

compositions (30%Ti and 70%Be in mass) were derived for the study: the composition with the minimum ($Be_{12}Ti$ min) and maximum ($Be_{12}Ti$ max) content of impurities and also the composition with the averaged content ($Be_{12}Ti$ "average"), Table 4. Therefore, the activation simulations with the irradiated $Be_{12}Ti$ should be performed for these three material compositions to address the uncertainty with the impurities fraction.

Table 4. Chemical compositions of $Be_{12}Ti$ with minimum, maximum and averaged impurities content, wt%.

Element	$Be_{12}Ti$ Min	$Be_{12}Ti$ Max	"Average"
Be	68.983 + 0.134	68.807 + 0.260	68.612 + 0.206
BeO	0.371	0.721	0.573
C	0.038	0.247	0.098
Fe	0.095	0.123	0.114
Al	0.005	0.035	0.019
Si	0.041	0.062	0.052
Mg	0.000	0.011	0.007
Zn	0.001	0.004	0.002
Cr	0.001	0.011	0.007
Ni	0.065	0.078	0.072
Cu	0.001	0.018	0.008
Ti	29.671	29.688	29.680
Zr	0.001	0.005	0.003
U	**0.00014**	**0.0105**	**0.0021**
Mn	0.000	0.005	0.003
Ag	0.000	0.004	0.002
Co	0.000	0.004	0.002
Pb	0.001	0.019	0.010
Ca	0.001	0.004	0.002
Mo	0.001	0.004	0.002
O	0.560 + 0.237	0.560 + 0.461	0.560 + 0.367
F	0.000	0.001	0.000
N	0.031	0.046	0.038
H	0.120	0.120	0.120
W	0.007	0.007	0.007
Na	0.001	0.001	0.001
Ta	0.001	0.001	0.001

2.4. $Be_{12}Ti$ Blocks

The manufacturing method for the $Be_{12}Ti$ blocks is based on the vacuum hot pressing of $Be_{12}Ti$ powder [8]. Because beryllides are very hard materials, electrical discharge machining was employed to cut out flat surfaces and holes to form hexagonal blocks with a material density of 2.25 g/cm^3 [8]. Shown in Figure 1 are the $Be_{12}Ti$ blocks assembled in a unit according to the latest consolidated design of the HCPB blanket [3].

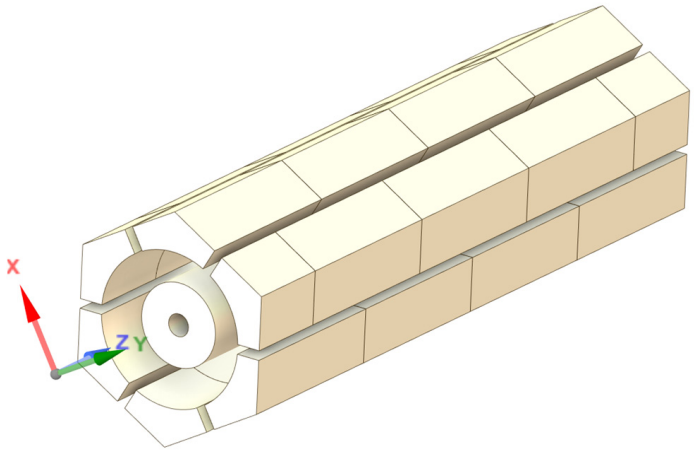

Figure 1. $Be_{12}Ti$ assembly for the latest consolidated HCPB breeder blanket design.

Radial cuts of the $Be_{12}Ti$ unit shown in Figure 1 were proposed to implement in the HCPB blanket design to reduce thermal stresses that take place during the warming up and cooling down cycles. Such radial segmentation of the $Be_{12}Ti$ unit can also be used for a mapping of the blocks in the blanket space to apply a practical classification of their properties after the thermal stresses and the neutron irradiation. This feature could be used in the future for the separate processing of the irradiated blocks to elaborate on a smart cycle with activated materials.

3. Modelling Methodology

3.1. HCPB Breeder Blanket Geometry Model

The HCPB blanket design based on the implementation of a Single Module Segmentation (SMS) conforms to the dimensions of the breeder blanket space in the generic DEMO CAD model for the DEMO baseline 2019 [12]. The blanket U-shaped first wall (FW) is 25 mm thick (20 mm in the HCPB blanket design 2017) and it is attached to a 150 mm thick back supporting wall (BSW), Figure 2. The blanket inner volume is subdivided into two parts separated by a back wall: a breeder zone (BZ) and a manifold. The manifold includes two big collectors for a He coolant and a small collector behind the back wall for a purge He gas. The BSW and gas collectors form the back supporting structure (BSS) of the HCPB blanket. The breeder units arranged in a hexagonal lattice, Figure 2, make up the breeder zone. The BZ is strengthened by radial central tubes of the breeder units ending with steel rods in the manifold region. The breeder ceramic annular layer, Figure 2, is surrounded by $Be_{12}Ti$ blocks forming a hexagonal pyramid (see Figure 1). Breeder ceramic pebbles (Li_4SiO_4 + 35% mol. Li_2TiO_3, 60% ^6Li enrichment) with 64% He volume fraction fill the cylindrical annual volume between the central feeding He pipe (∅ = 14 mm) and a separating pipe (∅ = 84 mm). A pressure (∅ = 94 outer, ∅ = 86 mm inner) and separating tubes form an annular gap for the outlet He coolant. The central and separating tubes have 2 mm thick walls. In the front part of the breeder ceramic layer, a $Be_{12}Ti$ annular insert (∅ = 52 mm, 127 mm length) is arranged to enhance a neutron multiplication here, Figure 2. All structural elements of the HCPB blanket are made by EUROFER steel.

The MCNP geometry model of the HCPB blanket was developed on the module base: the breeder blanket volume of the generic model is filled with the first level universe representing the empty blanket housing or box (FW plus the back supporting wall); this universe in turn is filled with the second level one representing manifolds and empty BZ. The MCNP geometry model of the HCPB DEMO represents 11.25° toroidal sector including 1 inboard breeder (IB), 1 outboard lateral (OBL) and a half of the central outboard (OBC) blankets, Figure 3. To simulate a 360° DEMO tokamak reflecting boundary surfaces were implemented in the model. The total number of the MCNP geometry cells containing $Be_{12}Ti$ is 425 and 410 in the IB and OBC blankets, respectively.

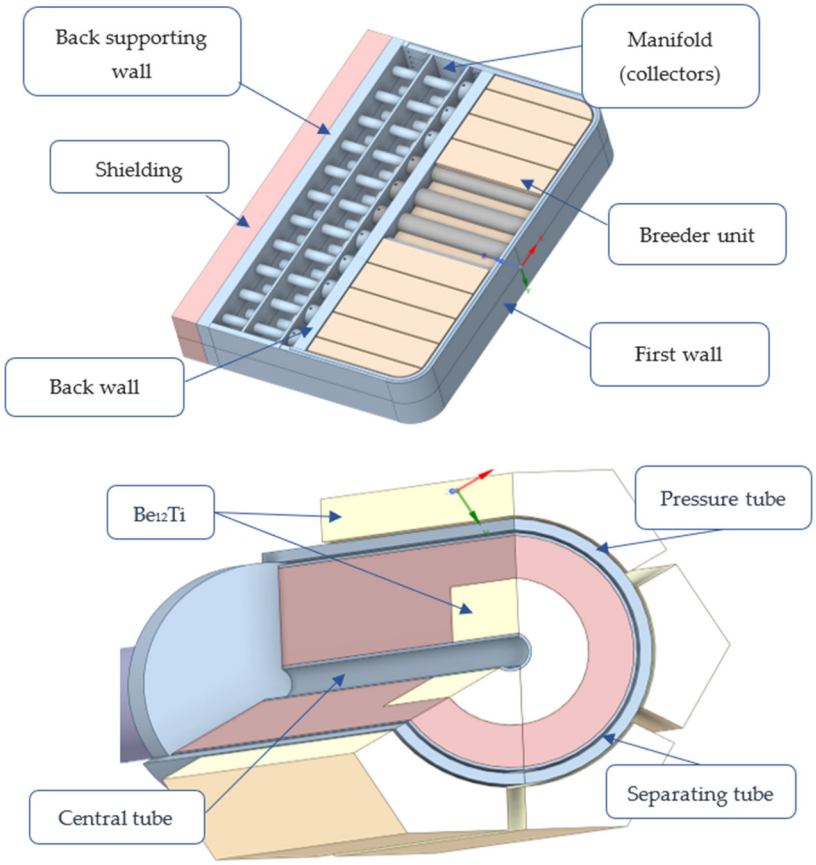

Figure 2. The layout of the HCPB breeder blanket: a horizontal slice (upper) and a breeder pin (bottom).

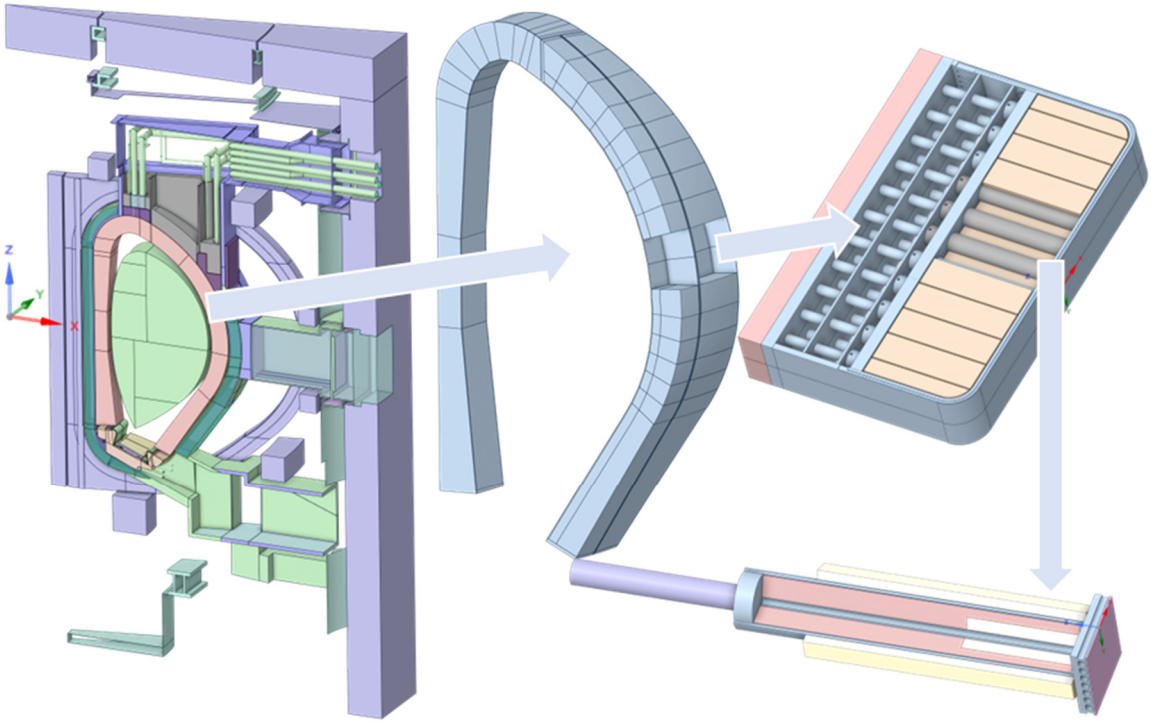

Figure 3. Geometry hierarchy of the modules in the MCNP geometry model.

3.2. Computer Codes and Nuclear Data

The activation simulations are performed in two steps: (1) a particle transport simulation to assess the neutron spectra in the different locations, (2) inventory calculations based on the neutron spectra to quantify the generation of the radioactive nuclides.

Step 1 in this procedure requires neutron spectra in all geometry cells where further activation analyses will be carried out. To this end, the set of the geometry cells of interest must be specified in the MCNP input file to tally the neutron spectra. Special attention should be paid to the accuracy of the nuclear responses. This can be achieved by applying the proper variance reduction technique, if necessary. Neutron flux intensities and spectra required for the activation analysis were computed with MCNP6.2 [13], making use of the HCPB DEMO geometry model described above, the CCFE 709 neutron energy group structure [14] to address a fine resonance structure in nuclear data at low-neutron energies and the JEFF-3.3 nuclear cross-section data [15]. In the present study, only the activation of the $Be_{12}Ti$ blocks was analyzed. Therefore, the tallying of the neutron spectra was performed in different geometry $Be_{12}Ti$ cells that belong to the different poloidal segments of the blanket structure. The statistical uncertainty in all calculations of the total neutron flux does not exceed 1%. For some low-energy bins, for instance, $1{\cdot}10^{-7}$~$1{\cdot}10^{-4}$ MeV, the relative error was calculated to be less ~10%. Normalization of the nuclear responses was carried out to the DEMO fusion nuclear power of 1998 MW, that results in a $7.094{\cdot}10^{20}$ s^{-1} neutron source intensity.

To facilitate the activation analyses, an interface code was developed and applied to numerous activation calculations. It makes use of the MCNP input file for neutron transport calculations as a main repository to obtain full information on materials used in the calculations. The interface assures a proper preparation and an execution of the big amount of the FISPACT II [14] inventory calculations according to the geometry cell numbers specified in the MCNP neutron transport calculations. The FISPACT II code involves a TENDL activation data library which is TENDL-2021 in the present version [16]. For the numerous activation calculations, the interface automatically prepares the FISPACT input files for each geometry cell using a proper fine material composition and the irradiation scenario. It then automatically submits a batch job for each geometry cell for an execution. The whole procedure is fully parallelized making use of an MPI technique. The inventory results of the FISPACT outputs are collected and processed by a versatile post-processing code.

3.3. DEMO Operational Scenario

The current baseline DEMO design [1] assumes two phases of the reactor operation [17]. In the first phase (5.2 calendar years), the arrangement of a so-called driver blanket is assumed with a goal to achieve a maximum displacement damage of 20 dpa in the steel contained in the first wall of the breeder blanket. During the second phase (14.8 calendar years), the second breeder blanket will be used in the reactor tokamak where the steel structure can withstand at least 50 dpa. This study only considered the first phase, because the blankets currently under design are planned to be the driver ones for the DEMO. According to the irradiation schedule [17], the first phase only covers the first 5.2 calendar years of operation. Figure 4 shows a graphical representation of the irradiation schedule used in the activation calculations. The first DEMO irradiation phase assumes 5.2 years minus 10 days of DEMO operation at a 30% load of the nominal fusion power followed by the pulsed operation with 48 pulses of 4 h at the 100% power and 1 h dwell time in between. This results in 1.57 full-power years of the DEMO operation and the breeder blanket neutron irradiation exposure.

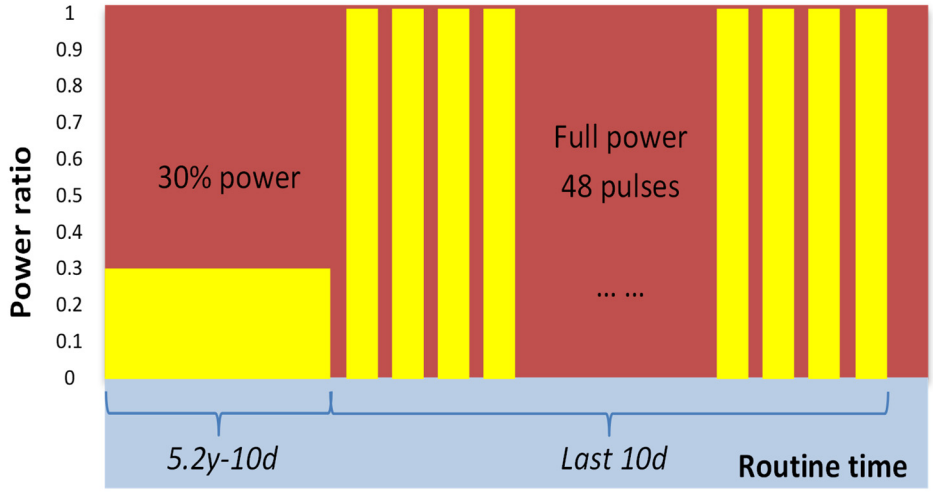

Figure 4. The DEMO operation scenario (1st phase).

4. Results of Activation Calculations

4.1. Activity of the $Be_{12}Ti$ in the HCPB Blankets

The activation calculations for the $Be_{12}Ti$ blocks were performed in the IB and OB blanket modules of the HCPB DEMO to assess total activity and decay heat making use of the different $Be_{12}Ti$ material definitions, Table 4. The DEMO tokamak is made up of 16 toroidal segments including 2 IB, 2 OBL and 1 OBC blankets. The total mass of the $Be_{12}Ti$ in the HCPB DEMO, ~600 tons, was calculated making use of the MCNP geometry model and the results for different blankets are listed in Table 5. This corresponds to ~270 m^3 of $Be_{12}Ti$ in the HCPB DEMO tokamak.

Table 5. Total mass of $Be_{12}Ti$ in the HCPB DEMO blankets (tons).

IB Blanket	Central OB Blanket	Lateral OB Blanket	Total Reactor
6.8	8.3	7.9	**603.2**

During the first phase of the DEMO operation (5.2 CY), the total activity of the $Be_{12}Ti$ accumulated in the HCPB OB blanket can achieve ~$5.52 \cdot 10^{17}$ Bq in the central outboard blanket ($Be_{12}Ti$ max) right after the reactor shutdown, Figure 5. The spread of the results for the different material compositions, specified in Table 4, does not exceed ~1% for cooling times up to 1 year. The activity of the $Be_{12}Ti$ drops down by a factor of ~50 one day and by the factor of ~500 one year after the shutdown of the reactor relative to the results right after the reactor shutdown. The difference of the results for the $Be_{12}Ti$ (max) and (min) is about the factor of 6 and 2 at the moments of 10 and 100 years after the reactor shutdown, respectively. The results do not include tritium activity assuming its full detritiation after the shutdown. The uncertainty of the FISPACT inventory results was assessed only for the cooling phase and it amounts to 3% at the short cooling times (less than 1 year) and it is up to ~10% for the cooling times exceeding 1 year. The representative results of the $Be_{12}Ti$ activity in the central outboard blanket (OBC) averaged over the $Be_{12}Ti$ volume for the cooling times from the shutdown to 100 years after are given in Table 6. The results discussed below in the text refer to the OBC blanket because the data for the lateral blanket are very close and the activity of the $Be_{12}Ti$ in the IB blanket is ~1.8 times less compared to the results for the OB blankets.

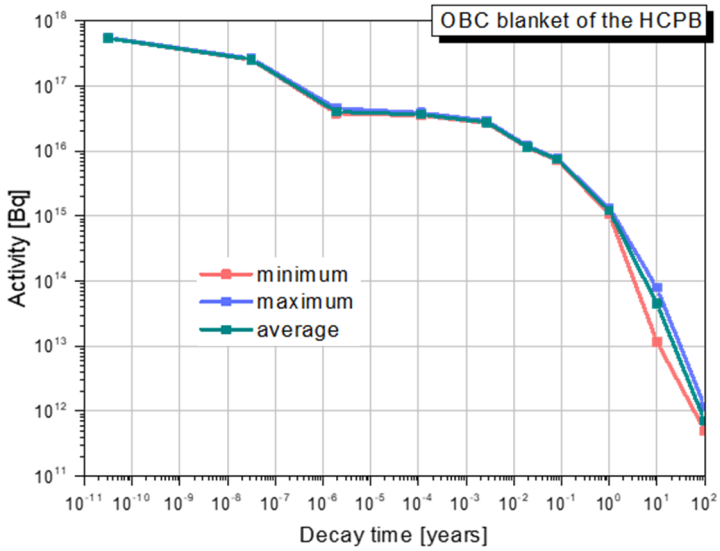

Figure 5. Activity of the $Be_{12}Ti$ for different material compositions in the central outboard blanket.

Table 6. Activity (Bq) of the $Be_{12}Ti$ in the central OB blanket of the HCPB DEMO.

$Be_{12}Ti$ Composition	Cooling Time							
	0	**1 s**	**1 h**	**1 Day**	**1 Month**	**1 Year**	**10 Years**	**100 Years**
Min	5.42×10^{17}	2.54×10^{17}	3.51×10^{16}	2.70×10^{16}	7.21×10^{16}	1.07×10^{15}	1.17×10^{13}	5.02×10^{11}
Average	5.44×10^{17}	2.57×10^{17}	3.62×10^{16}	2.76×10^{16}	7.42×10^{15}	1.21×10^{15}	4.51×10^{13}	7.12×10^{11}
Max	5.53×10^{17}	2.65×10^{17}	3.89×10^{16}	2.91×10^{16}	7.65×10^{15}	1.35×10^{15}	7.89×10^{13}	1.17×10^{12}

The results for the decay heat power density in the $Be_{12}Ti$ of the OB central blanket with different material specifications, Table 4, are presented in Figure 6. For the cooling time of up to 30 days, the decay heat power density for $Be_{12}Ti$ with different impurities content differ insignificantly. After 100 years of cooling, the difference in the power density for the materials with minimum and maximum impurity concentrations reaches a factor of ~50. The power density right after the reactor shutdown is ~40 kW/m^3 and it drops down by a factor ~100 30 days later.

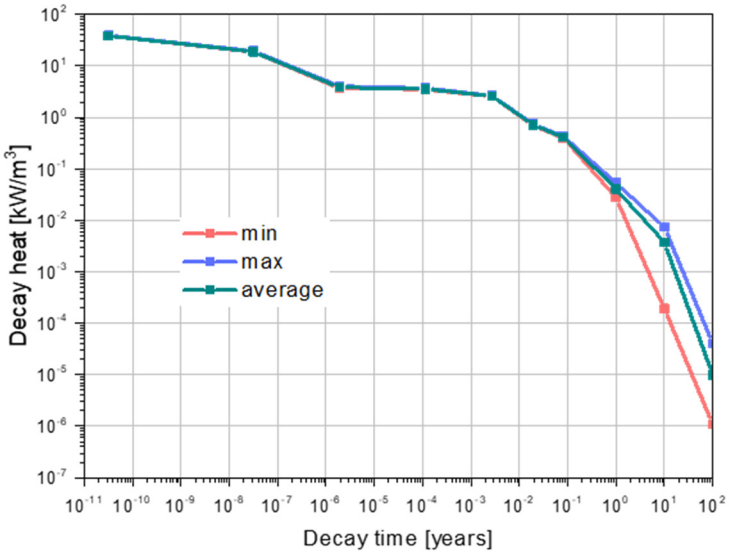

Figure 6. Decay heat power density in the OBC blanket.

The tritium production in $Be_{12}Ti$ through $^{9}Be(n,t)^{8}Li$ reaction represents a potential danger in the handling procedure of any irradiated material including pure beryllium. Due to zero retention at high-operation temperatures [18], tritium is assumed to be removed from the $Be_{12}Ti$ blocks with the He purge gas in the HCPB blanket [3] and therefore tritium activity is not accounted for in the present results (the results are nevertheless available). The tritium generation due to the fusion neutron irradiation of Ti is negligible and does not noticeably affect the activation of the $Be_{12}Ti$. The tritium retention in the $Be_{12}Ti$ tends to be zero at temperatures above 600 °C and it goes up at lower temperatures [18]. The current HCPB blanket layout assumes that the $Be_{12}Ti$ block is warmed up to ~800 °C in the regions close to the first wall and up to ~530 °C in the rear part of the breeder zone [3]. Due to an uncertainty of the experimental data [18], it is likely that some parts of the $Be_{12}Ti$ assembly with not high enough temperatures could theoretically retain some tritium amount. This option is not considered in the current work.

The breakdown of the total activity of the $Be_{12}Ti$ ("average") in the central outboard blanket (OBC) is shown in Figure 7. Assuming that a remote handling of the "hot" blankets after the reactor shutdown might be possible after a specific cooling time, isotopes dominating the total activity at the cooling time longer than 1 month were determined and the breakdown of the total activity is presented in Figure 7. For the cooling time from 1 month to 1 year, ^{45}Ca ($T_{1/2}$ = 162.6 days) and ^{46}Sc ($T_{1/2}$ = 83.8 days) define the total activity. These isotopes are formed during the neutron irradiation of Ti due to (n,p) and (n,α) reactions. ^{60}Co ($T_{1/2}$ = 5.27 years) dominates the activity 10 years after the shutdown of the reactor; it is formed from the Co impurity in the $Be_{12}Ti$ due to $^{59}Co(n,\gamma)^{60}Co$ reaction. The decay of ^{63}Ni defines the activity for the cooling time of 100 years. The significant concentration of ^{63}Ni($T_{1/2}$ = 100 years) in the $Be_{12}Ti$ results from the accumulation of this isotope due to the reaction on the Ni impurity, $^{62}Ni(n,\gamma)^{63}Ni$.

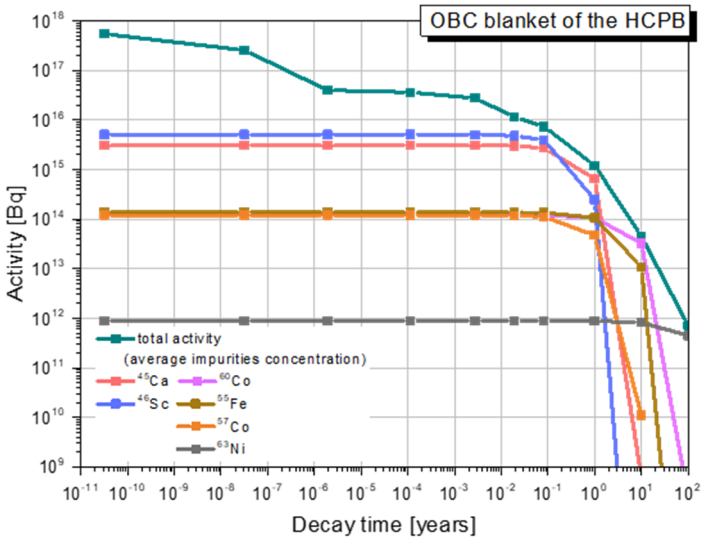

Figure 7. The dominant radionuclides in the irradiated Be12Ti in the OB central blanket at the cooling time longer than 1 month.

A time evolution of the specific activity in the irradiated $Be_{12}Ti$ of the different newly generated radioactive nuclides in the central OB blanket grouped according to atomic numbers is shown in Figure 8. The tritium removal bypass is switched off in the FISPACT activation simulation but tritium generation is not accounted for in the final result. Using the data presented in Figure 8, several groups of activated products responsible for the $Be_{12}Ti$ activity can be identified according to their atomic numbers. Right after the reactor shutdown, a variety of radionuclides with a wide spread of atomic numbers are generated: light ones with A < 14, 18 < A < 30, 30 < A < 65 including fission products, 71 < A < 76, 80 < A < 82 and fissile nuclides with 90 < A< 97. One year after the shutdown, the main contributors to the activity are still nuclides with 18 < A < 30, some elements within the wide

group of the fission products, Ta-W-Re, Tl and the group of the trans uranium elements: U, Pu and Am. After 100 years of decay, the most essential elements are N, Ni, Cd, U, Pu and Am. The chemical impurities available in the $Be_{12}Ti$ affect and form its activity for all cooling times.

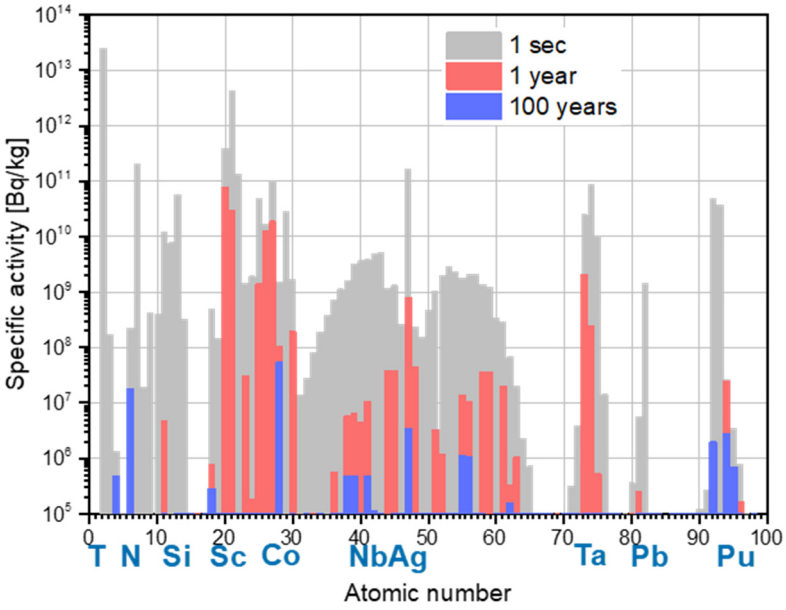

Figure 8. Time evolution of the generated radioactive nuclides.

4.2. Disposal Options for the $Be_{12}Ti$

4.2.1. Total Disposal Limits

Each country with a current or future nuclear waste busyness develops different approaches to the handling of the nuclear waste: disposal, storage and recycling. Many countries are engaged in the elaboration of projects for the long-term disposal of radioactive wastes. The disposal facilities are developed to be operated on over many decades to keep their functionality up to hundreds of years. According to IAEA classification [19], radioactive waste is divided into very low (VLLV), low (LLW), intermediate (ILW) and high-level waste (HLW). The exact definition for the waste in each class differs from country to country. Two different methodologies for waste regulations are being applied to different repositories [20]: global activity limits to classify waste and limits on the accumulated individual radionuclides. A United Kingdom (UK) regulator employs global activity limits, France and Germany have adopted the limits for chosen isotopes, and Spanish and USA regulations assume limits for the nuclides additionally grouped in subclasses. The repository capacities in several countries for LLW (or near-surface disposal) waste are presented in Table 7 [21]. Compared to the $Be_{12}Ti$ volume in the HCPB blankets of ~270 m^3, the available disposal capacities could be sufficient for its arrangement in a case of such decision.

Table 7. The sizes of the repositories for LLW, [m^3].

Country, Repository Name	Repository Capacity
United Kingdom, LLWR	1,800,000
France, L'Aube	1,000,000
Spain, El Cabril	36,000
Japan, Rokkasho	600,000
Finland, VLJ Oilkiluoto	8000
Sweden, SFR	266,000

The UK waste regulator applies global activity limits subdividing them into classes: maximum α-activity and $\beta + \gamma$ activities with the upper limits of 4 MBq/kg and 12 MBq/kg, respectively [22,23]. The LLW criteria adopted in the Spanish regulations (low and intermediate level waste LILW limit level 1, El Cabril facility) amount to 0.185 MBq/kg and 37 MBq/kg for the α and $\beta + \gamma$ activities, respectively [24–27].

Shown in Figure 9 is the specific $\beta + \gamma$ activity of the $Be_{12}Ti$ in the OBC blanket for three different material definitions (Table 3) compared to the available disposal limits. Respectively, the α-activity of the irradiated $Be_{12}Ti$ is presented in Figure 10. The big spread of the results for the α-activity comes from the wide range of the uranium impurity concentration for different material compositions, Table 4. The data shown in Figures 9 and 10 do not indicate the disposal opportunity for the irradiated neutron multiplier of the HCPB blankets in the repositories of UK and Spain due to the high $\beta + \gamma$ activity. In case of an isotope separation procedure applied to the irradiated $Be_{12}Ti$, some disposal options could be considered for the α-radioactive nuclides.

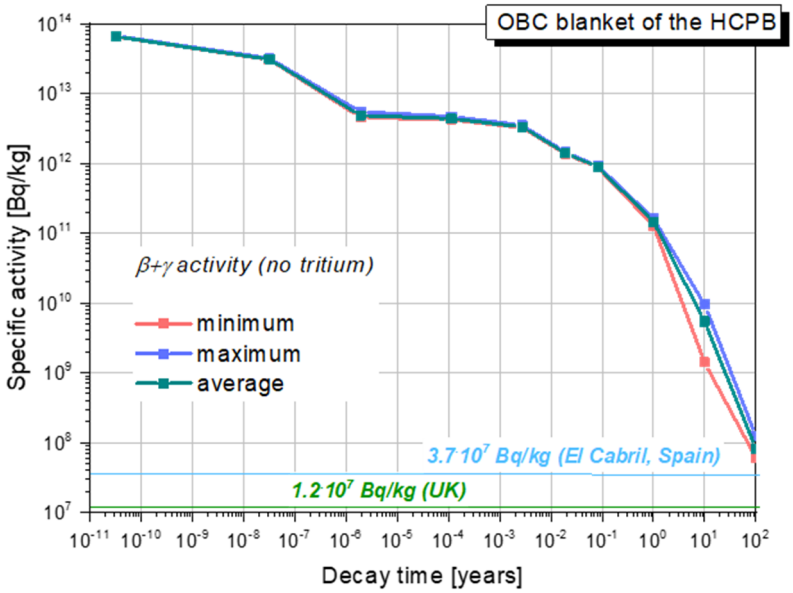

Figure 9. Specific $\beta + \gamma$-activity of the $Be_{12}Ti$ in the central OB blanket of the HCPB DEMO.

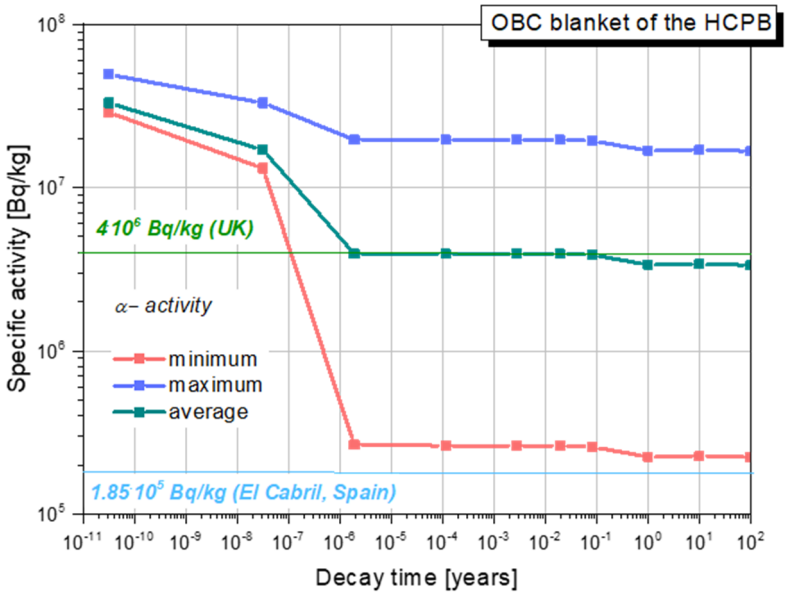

Figure 10. Specific α-activity of the $Be_{12}Ti$ in the central OB blanket of the HCPB DEMO for different material compositions.

4.2.2. Radionuclide-Specific Limits

Alternative to the total limits, the radionuclide-specific LLW limits operate with the data for separate radioactive isotopes that can be disposed in the dedicated radioactive waste repositories. The main difference between repositories is their depth. Two disposal opportunities are considered in this work: above ground (Centre de l'Aube in France, El Cabril in Spain, USA) and below ground (Konrad in Germany). The limits adopted in each country for the acceptance of the LLA disposal differ and they are defined by specific safety and technical requirements applied to the repositories.

Listed in Table 8 are the results for the accumulated specific activities for separated radionuclides in the irradiated $Be_{12}Ti$ ("average" material composition) in the OBC blanket for different cooling times compared to the French maximum LLW acceptance limits for the Centre Stockage de l'Aube (CSA) disposal facility in France [22,28–32]. For the cooling time beyond 1 year, the activities of the accumulated isotopes do not exceed the LLW limits specified in Table 8 except ^{108m}Ag ($T_{1/2}$=418 years). This isotope is produced as a result of the $^{107}Ag(n,\gamma)^{108m}Ag$ reaction due to Ag impurity in the $Be_{12}Ti$ and its activity exceeds the facility limit during the whole cooling time. In case of the $Be_{12}Ti$ (min), material composition accumulation of this isotope is not expected, purification of the $Be_{12}Ti$ ("average" and max) and extraction of the Ag impurity seems to be expensive and it is beyond the scope of this work. The fission products listed in Table 8 are not a safety issue, neither in the short term nor for the long-term waste disposal strategy. The volatile fission products such as ^{129}I also do not represent a risk for inhalation.

Table 8. Accumulated activity of various radioactive isotopes in the central OB blanket compared to the French nuclear waste regulations.

Radionuclide	LLW Limit (Bq/kg)	$Be_{12}ti$ Activity (bq/kg)		
		1 Year	10 Years	100 Years
Sn-126	2.70×10^3	1.07×10^2	1.07×10^2	1.07×10^2
Cl-36	5.00×10^3	2.94×10^1	2.94×10^1	2.94×10^1
Nb-94	1.20×10^5	5.76×10^2	5.76×10^2	5.74×10^2
Th-232	1.10×10^6	6.50×10^{-6}	6.50×10^{-6}	6.50×10^{-6}
Ag-108m	1.40×10^6	***3.73 × 10^6^***	***3.68 × 10^6^***	***3.17 × 10^6^***
I-129	1.40×10^6	5.16×10^0	5.16×10^0	5.16×10^0
Be-10	5.10×10^6	4.81×10^5	4.81×10^5	4.81×10^5
Zr-93	1.80×10^7	8.99×10^2	8.99×10^2	8.99×10^2
Mo-93	3.80×10^7	1.17×10^5	1.13×10^5	1.11×10^5
Tc-99	4.40×10^7	1.13×10^4	1.13×10^4	1.04×10^4
Se-79	5.50×10^7	9.47×10^0	9.47×10^0	9.46×10^0
C-14	9.20×10^7	1.78×10^7	1.78×10^7	1.78×10^7
Ni-59	1.10×10^8	7.98×10^5	7.98×10^5	7.88×10^5
H-3	2.00×10^8	-	-	-
Cs-135	2.60×10^8	1.75×10^2	1.75×10^2	1.75×10^2
Ca-41	3.00×10^8	3.72×10^3	3.72×10^3	3.72×10^3
Pd-107	3.00×10^8	2.69×10^1	2.69×10^1	2.69×10^1
Cs-137	3.30×10^8	1.13×10^7	9.20×10^6	1.15×10^6
Sn-121m	3.70×10^8	1.62×10^4	1.40×10^4	3.39×10^3

Table 8. *Cont.*

Radionuclide	LLW Limit (Bq/kg)	Be_{12}ti Activity (bq/kg)		
		1 Year	10 Years	100 Years
Sm-151	4.50×10^{8}	3.39×10^{5}	3.16×10^{5}	1.58×10^{5}
Ni-63	3.20×10^{9}	1.06×10^{8}	9.93×10^{7}	5.34×10^{7}
Sr-90	6.00×10^{9}	5.30×10^{6}	4.27×10^{6}	4.89×10^{5}
Eu-154	5.80×10^{10}	2.15×10^{5}	1.04×10^{5}	7.36×10^{1}
Eu-152	7.50×10^{10}	5.24×10^{3}	3.30×10^{3}	3.28×10^{1}
Ce-144	8.80×10^{10}	3.55×10^{7}	1.21×10^{4}	-
Ru-106	1.20×10^{11}	3.78×10^{7}	8.36×10^{4}	-
Ag-110m	1.20×10^{11}	7.37×10^{8}	8.15×10^{4}	-
Na-22	1.30×10^{11}	5.79×10^{6}	4.36×10^{5}	5.78×10^{-5}
Co-60	1.30×10^{11}	1.28×10^{10}	3.92×10^{9}	3.02×10^{4}
Cs-134	1.90×10^{11}	2.70×10^{6}	1.31×10^{5}	1.58×10^{-7}
Mn-54	3.60×10^{11}	1.42×10^{9}	9.64×10^{5}	-
Sb-125	5.10×10^{11}	3.31×10^{6}	3.46×10^{5}	1.38×10^{-4}
Pm-147	5.80×10^{11}	2.04×10^{7}	1.89×10^{6}	2.92×10^{-4}
Zn-65	6.00×10^{11}	1.95×10^{8}	1.75×10^{4}	-
Sn-119m	1.40×10^{12}	6.77×10^{3}	2.86×10^{0}	-
Tl-204	3.30×10^{12}	2.453×10^{5}	4.88×10^{4}	4.42×10^{-3}
Fe-55	6.10×10^{12}	1.28×10^{10}	1.31×10^{9}	4.46×10^{-1}

The Spanish national regulator also applies the radionuclide-specific criteria but it splits them into three subgroups: VLLW—very low-level waste and LILW—low–intermediate-level waste group 1 and 2. Presented in Table 9 are the waste acceptance limits for several isotopes adopted for the El Cabril disposal facility [25,26,32]. The LILW-1 level needs verification of a waste container resistance to compression and immersion with a certification for a possible diffused liquid release. The LILW-2 level must satisfy limits to leaching and thermal cycles. Both LILW levels assume homo- and heterogeneous waste incorporated or immobilized in a solid matrix. The specific activity of ^{60}Co and ^{137}Cs accumulated in the irradiated Be_{12}Ti could be an issue for the long-term storage in the El Cabril depository in case of the use of the container certified for the LILW-1 limit. In case of the Be12Timax composition, Table 2, the specific activities of these isotopes also do not exceed the El Cabril LILW-2 limits: $2.5 \cdot 10^{10}$ and $5.7 \cdot 10^{7}$ Bq/kg for ^{60}Co and ^{137}Cs, respectively. The total activity accumulated in the Be_{12}Ti of the HCPB breeder blankets 1 year after the shutdown compared to the installed capacity of the El Cabril facility [33] is presented in Table 10. The total activity of ^{14}C accumulated in the HCPB tokamak is about a half of the total capacity of the El Cabril facility for this radionuclide and it seems to be too high for the disposal there. The entire or partial disposal in the El Cabril depository of the irradiated Be_{12}Ti could be nevertheless feasible.

Table 9. Accumulated activity of various radioactive isotopes in the central OB blanket compared to the Spanish nuclear waste regulations.

Radionuclide	LILW-1 (Bq/kg)	LILW-2 (Bq/kg)	$Be_{12}Ti$ Activity (Bq/kg)		
			1 Year	10 Years	100 Years
Co-60	3.7×10^6	5.0×10^{10}	1.28×10^{10}	3.92×10^9	3.02×10^4
H-3	7.4×10^6	1.0×10^9	-	-	-
Cs-137	3.7×10^6	3.3×10^8	1.13×10^7	9.20×10^6	1.15×10^6
Nb-94	1.2×10^5	1.2×10^5	5.76×10^2	5.76×10^2	5.74×10^2
Ni-59	1.9×10^7	6.3×10^7	7.98×10^5	7.98×10^5	7.88×10^5
Ni-63	3.6×10^9	1.2×10^{10}	1.06×10^8	9.93×10^7	5.34×10^7
C-14	6.1×10^7	2.0×10^8	1.78×10^7	1.78×10^7	1.78×10^7
Tc-99	3.0×10^5	1.0×10^6	1.13×10^4	1.13×10^4	1.04×10^4

Table 10. Total radionuclide accumulation in the $Be_{12}Ti$ of the HCPB DEMO 1 year after the shutdown compared to the reference inventory (Bq) of the El Cabril disposal facility.

Radionuclide	El Cabril	$Be_{12}Ti$			
		IB	OBC	OBL	Tokamak
H-3	2.0×10^{14}	-	-	-	-
C-14	2.0×10^{13}	9.1×10^{10}	1.5×10^{11}	1.5×10^{11}	1.0×10^{13}
Ni-59	2.0×10^{14}	4.2×10^9	6.6×10^9	6.5×10^9	4.3×10^{11}
Ni-63	2.0×10^{15}	5.6×10^{11}	8.8×10^{11}	8.7×10^{11}	6.0×10^{13}
Co-60	2.0×10^{18}	7.0×10^{13}	1.1×10^{14}	1.1×10^{14}	7.5×10^{15}
Sr-90	2.0×10^{17}	2.6×10^{10}	4.4×10^{10}	4.4×10^{10}	2.9×10^{12}
Nb-94	1.0×10^{12}	2.5×10^6	4.8×10^6	4.8×10^6	3.1×10^8
Tc-99	3.2×10^{12}	5.9×10^7	9.4×10^7	9.3×10^7	6.4×10^9
I-129	1.5×10^{11}	2.5×10^4	4.3×10^4	4.3×10^4	2.9×10^6
Cs-137	3.7×10^{15}	5.5×10^{10}	9.4×10^{10}	9.4×10^{10}	6.3×10^{12}

Within a KONEKT research project [34], repository options for the irradiated beryllium were analyzed to assess possibilities of its storage in Germany. A total mass of the irradiated Be already disposed in different institutions and locations in Germany is estimated to be ~3000 kg [34]. The assessment of the safety issues of the $Be_{12}Ti$ activation results produced in this report is performed making use of the facility limits available for the Konrad mine repository. Although this repository is big enough to arrange millions of tons of radioactive materials, its capacity for the storage of the radioactive Be is limited to 24.5 kg (Table 12 [35]) because of the potential danger of groundwater contamination. A theoretical option for the $Be_{12}Ti$ secure disposal in the steel container of Type I [35] with a useful volume of 3.9 m^3 was chosen for the comparison assuming the limits for the waste group APG03 (metal products, Tables 5 and 6 [35]). Presented in Table 11 are the results for the activity of the accumulated isotopes in the irradiated $Be_{12}Ti$ ("average") 1 year after the reactor shutdown compared to the Konrad facility limits. The available results for tritium accumulation are not included in Table 11 because the full tritium removal from the irradiated $Be_{12}Ti$ blocks is foreseen and expected in the HCPB blankets as it is pointed out above. The accumulated activities of ^{60}Co (produced from Co impurity) and ^{46}Sc (produced from the Ti irradiation) exceed the Konrad limits by the factor of ~10. The results for ^{45}Ca and ^{57}Co slightly exceed the limits. In case of several years of decay for ^{46}Sc, ^{45}Ca and ^{57}Co isotopes, the safety limits

for their disposal can be reliably secured. In the case of the ^{60}Co storage in the Konrad repository, the decay time of several decades is necessary to meet the safety requirements.

Table 11. Accumulated activity of various radioactive isotopes in the central OB blanket compared to the German nuclear waste regulations for the Konrad repository.

Isotope	Limit, Bq/m^3	Activity, Bq/m^3	Isotope	Limit, Bq/m^3	Activity, Bq/m^3
Be-10	1.0×10^{12}	1.1×10^{9}	H-3	6.9×10^{14}	-
Cl-36	1.0×10^{12}	6.7×10^{4}	C-14	8.7×10^{12}	4.1×10^{10}
Ar-39	2.1×10^{12}	8.2×10^{8}	Na-22	2.8×10^{12}	1.1×10^{10}
Ca-41	6.4×10^{11}	8.5×10^{6}	S-35	9.7×10^{13}	3.7×10^{5}
Fe-55	1.1×10^{15}	2.9×10^{13}	Ca-45	1.6×10^{14}	***1.8 × 10^{14}***
Co-60	2.0×10^{12}	***2.9 × 10^{13}***	Sc-46	7.9×10^{12}	***6.8 × 10^{13}***
Ni-63	2.8×10^{13}	2.4×10^{11}	V-49	2.2×10^{15}	7.0×10^{10}
Rb-87	1.4×10^{12}	3.8×10^{0}	Cr-51	8.2×10^{14}	4.3×10^{8}
Nb-94	1.9×10^{11}	1.3×10^{6}	Mn-54	1.2×10^{13}	3.2×10^{12}
Ag-108m	1.0×10^{12}	8.5×10^{9}	Co-57	1.2×10^{13}	***1.3 × 10^{13}***
Sn-126	1.3×10^{12}	2.5×10^{5}	Co-58	1.8×10^{13}	1.2×10^{12}
Cs-137	3.3×10^{12}	2.6×10^{10}	Fe-59	1.4×10^{13}	1.8×10^{9}
Pb-210	5.6×10^{11}	4.8×10^{1}	Ni-59	3.8×10^{13}	1.8×10^{9}
Ra-226	1.8×10^{10}	3.9×10^{0}	Zn-65	1.8×10^{13}	4.5×10^{11}
Ac-227	9.7×10^{10}	3.0×10^{1}	Se-79	6.7×10^{12}	2.2×10^{4}
Ra-228	1.4×10^{11}	1.7×10^{-1}	Kr-85	1.6×10^{13}	1.3×10^{9}
Th-230	7.4×10^{9}	2.5×10^{3}	Sr-89	3.6×10^{13}	1.0×10^{9}
Pa-231	7.7×10^{9}	3.4×10^{2}	Sr-90	2.6×10^{12}	1.2×10^{10}
Th-232	5.1×10^{9}	1.5×10^{-2}	Nb-93m	1.3×10^{14}	1.1×10^{8}
U-233	6.9×10^{9}	2.5×10^{3}	Mo-93	3.1×10^{13}	2.6×10^{8}
U-234	1.0×10^{10}	6.0×10^{5}	Zr-93	4.1×10^{12}	2.1×10^{6}
U-235	5.6×10^{9}	2.5×10^{4}	Nb-95	3.1×10^{13}	2.3×10^{10}
Np-237	1.3×10^{10}	1.2×10^{6}	Zr-95	2.2×10^{13}	1.1×10^{10}
U-238	2.0×10^{10}	5.6×10^{5}	Tc-99	3.1×10^{12}	2.6×10^{7}
Pu-238	3.3×10^{11}	1.9×10^{9}	Ru-103	4.4×10^{13}	7.2×10^{8}
Am-242m	1.4×10^{10}	2.1×10^{6}	Ru-106	5.4×10^{12}	8.6×10^{10}
Pu-244	1.8×10^{10}	4.7×10^{-5}	Pd-107	2.0×10^{13}	6.2×10^{4}
Cm-245	3.3×10^{10}	2.7×10^{1}	Cd-109	7.9×10^{13}	1.0×10^{11}
Cm-247	1.4×10^{10}	2.2×10^{-7}	Ag-110m	3.8×10^{12}	1.7×10^{12}
Cm-248	1.2×10^{10}	8.1×10^{-8}	Cd-113m	1.3×10^{13}	3.7×10^{6}
			I-125	1.1×10^{14}	4.0×10^{2}
			Sb-125	9.7×10^{12}	7.6×10^{9}
			Te-125m	1.4×10^{14}	1.8×10^{9}
			I-129	2.6×10^{12}	1.2×10^{4}
			Ba-133	7.9×10^{12}	2.9×10^{5}
			Cs-134	4.1×10^{12}	6.2×10^{9}
			Cs-135	3.6×10^{12}	4.0×10^{5}
			Ce-144	7.4×10^{12}	8.1×10^{10}

The classification of waste for near-surface disposal in the USA supposes three classes: A, B and C [36]. The waste of class A must satisfy the minimum safety requirements and it includes mildly contaminated waste products (trash, clothing, etc.). The waste of classes B and C can be applied to nuclear reactor facilities, exhausted radioactive sources, etc. Class B must meet rigorous requirements to ensure stability after disposal. Class C assumes not only rigorous requirements and provides stability but also it must assure protection against inadvertent intrusion [36]. The specific activity of several long-lived radioactive isotopes ($T_{1/2}$ > 5 years) in the irradiated $Be_{12}Ti$ of the OBC blanket after 1 year of the cooling time is displayed in Table 12 compared to the limits for different classes of the LLW in the USA. Class B is not used in this specification. The results for the short-lived isotopes ($T_{1/2}$ < 5 years) 1 year after the shutdown are presented in Table 13. The disposal of the irradiated $Be_{12}Ti$ could likely be feasible in the USA near-surface facilities. The concentrations of ^{241}Pu and ^{60}Co are not a hindrance for the storage of the irradiated $Be_{12}Ti$ because the limits and corresponding measures for class B or C should then be applied for the containers.

Table 12. Specific activity (Bq/m^3) of several *long-lived* radionuclides in the $Be_{12}Ti$ compared to the limits for the different classes of LLW in the USA [36].

Radionuclide	Class A	Class C	$Be_{12}Ti$
C-14 in activated metal	2.96×10^{11}	Class A × 10	4.1×10^{10}
Ni-59 in activated metal	8.14×10^{11}	Class A × 10	1.8×10^{9}
Nb-94 in activated metal	7.40×10^{8}	Class A × 10	1.3×10^{6}
Tc-99	1.11×10^{11}	Class A × 10	2.6×10^{7}
I-129	2.96×10^{8}	Class A × 10	1.2×10^{4}
Pu-241	1.30×10^{4} [1]	Class A × 10	2.2×10^{4} [1]
Cm-242	7.40×10^{4} [1]	Class A × 10	1.7×10^{2} [1]

[1] Units are Bq/g.

Table 13. Specific activity (Bq/m^3) of several *short-lived* radionuclides in the $Be_{12}Ti$ compared to the limits for the different classes of LLW in the USA.

Radionuclide	Class A	Class B	Class C	$Be_{12}Ti$
H-3	1.5×10^{12}	([1])	([1])	-
Co-60	2.6×10^{13}	([1])	([1])	2.9×10^{13}
Ni-63 in activated metal	1.3×10^{12}	2.6×10^{13}	2.6×10^{14}	2.4×10^{11}
Sr-90	1.5×10^{9}	5.6×10^{12}	2.6×10^{14}	1.2×10^{10}
Cs-137	3.7×10^{10}	1.6×10^{12}	1.7×10^{14}	2.6×10^{10}

[1] There are no limits established for this radionuclide in Class B or C wastes. This waste shall be Class B unless the concentrations of other nuclides in this determine the waste to Class C independent of these nuclides.

4.2.3. Location Dependent Processing of the Irradiated $Be_{12}Ti$ Blocks

The prismatic $Be_{12}Ti$ unit has a radial length of ~42 cm in the outboard blankets in the reactor mid plane, Figure 1. Because of the block structure of this unit, there could be an opportunity to process the differently located $Be_{12}Ti$ blocks under the strict remote control. This enables the special treatment of the irradiated blocks located in the different radial positions in the $Be_{12}Ti$ assembly making use of a remote handling technique. Figure 11 displays the results for the β+γ-specific activity of the $Be_{12}Ti$ assembly ("average" material composition) arranged in the OBC blanket for two radial segments: a front zone (close to FW) of ~26 cm length and a rear zone of ~16 cm (close to back wall). The results averaged over the total volume of the $Be_{12}Ti$ in the OBC blanket ("average", Figure 9) are also presented for the comparison. One year after the reactor shutdown, the specific activity for the front zone is higher by ~35% and that for the rear zone is lower by ~70% compared to the "average" results. Due to the FW neutron wall-loading profile, the upper, central and bottom parts of the blanket are exposed to the different neutron fluxes; in the mid plane of the reactor, the neutron flux is at a maximum. To assess the difference of the results for these parts, the specific activity was calculated in the highest, central and lowest locations in the front zone of the $Be_{12}Ti$ assemblies (26 cm length). The β+γ-specific activity in the "front" part of the $Be_{12}Ti$ assemblies 1 year after the reactor shutdown in the upper and bottom parts of the blanket are lower compared to the central part by ~15% and ~23%, respectively. The results indicate a significant difference for the specific activity of the $Be_{12}Ti$ along the radial distance from the FW. The poloidal distribution of the activity along the blanket height is not so large. In case of the disposal possibility, the irradiated $Be_{12}Ti$ blocks could be processed separately using a "layer by layer" approach to find the best processing strategy.

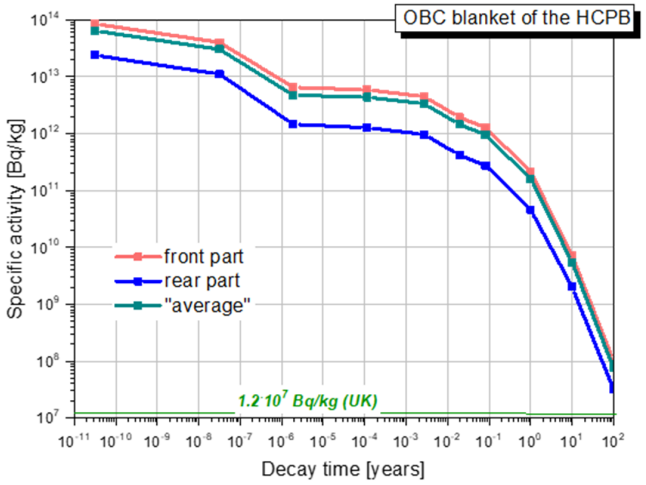

Figure 11. β+γ-specific activity of the two radial layers of the Be12Ti in the OB central blanket.

4.3. Dominant Radionuclides

The detailed breakdown of the generated activity and dose rates due to inhalation for different cooling times is given in Table 14. The results were obtained with $Be_{12}Ti$ "average" material composition in the central OB blanket and they do not include the data for tritium accumulation due to its removal from the blanket with the purge gas. The threshold for the inclusion of the isotopes in the table is ~0.5% from the total activity or dose rate. The short-term activity of the $Be_{12}Ti$ is dominated by Sc and Ca isotopes accumulated through (*n,xpxn*) reactions on Ti isotopes. Therefore, the inherent presence of these isotopes in the radioactive wastes has to be tolerated and the waste handling should account for this issue. The long-term activity of the $Be_{12}Ti$ is formed mainly by the nuclear reaction products coming from the neutron irradiation of the impurities available in the initial material. To some extent, this issue could be managed through (a) the purification of the Be and Ti used for the $Be_{12}Ti$ production and (b) through the use of more "pure" materials such as $Be_{12}Ti$ from the Ulba factory, Table 2. At the very long-cooling storage time (>100 years), the fissile isotopes and fission products also appear in the group of the dominating isotopes.

Table 14. Dominant radionuclide in the $Be_{12}Ti$ of the OBC blanket responsible for activity and dose rates (inhalation) for different cooling times.

Isotope	Activity, Bq/kg	Isotope	Dose Rate Inhalation, %
		1 s	
He-6	2.52×10^{13}	Sc-46	3.80×10^{1}
Sc-48	2.22×10^{12}	Sc-48	2.23×10^{1}
Sc-47	7.54×10^{11}	Ca-45	1.25×10^{1}
Sc-46	6.12×10^{11}	Sc-47	5.04×10^{0}
Sc-46m	4.82×10^{11}	Co-60	4.14×10^{0}
Ca-45	3.71×10^{11}	Pu-239	2.19×10^{0}
N-16	2.03×10^{11}	Ta-182	1.72×10^{0}
Ag-110	1.31×10^{11}	He-6	1.68×10^{0}
		Xe-133	1.53×10^{0}
		Sn-130	1.03×10^{0}
		Sn-129m	8.55×10^{-1}
		Pu-238	8.39×10^{-1}
		Tc-105	7.01×10^{-1}
		Sn-129	6.81×10^{-1}
		Pu-241	4.77×10^{-1}

Table 14. *Cont.*

Isotope	Activity, Bq/kg	Isotope	Dose Rate Inhalation, %
	1 h		
Sc-48	2.18×10^{12}	Sc-46	4.12×10^{1}
Sc-47	7.48×10^{11}	Sc-48	2.38×10^{1}
Sc-46	6.11×10^{11}	Ca-45	1.36×10^{1}
Ca-45	3.71×10^{11}	Sc-47	5.41×10^{0}
W-187	7.58×10^{10}	Co-60	4.49×10^{0}
Sc-49	5.14×10^{10}	Pu-239	2.37×10^{0}
Np-239	3.71×10^{10}	Ta-182	1.86×10^{0}
Mn-56	3.51×10^{10}	Xe-133	1.66×10^{0}
Ti-45	3.42×10^{10}	Pu-238	9.09×10^{-1}
Co-58m	2.03×10^{10}	Pu-241	5.17×10^{-1}
		Xe-135	4.88×10^{-1}
	1 day		
Sc-48	1.51×10^{12}	Sc-46	4.52×10^{1}
Sc-47	6.17×10^{11}	Sc-48	1.83×10^{1}
Sc-46	6.07×10^{11}	Ca-45	1.50×10^{1}
Ca-45	3.69×10^{11}	Co-60	4.96×10^{0}
W-187	3.88×10^{10}	Sc-47	4.93×10^{0}
Np-239	2.80×10^{10}	Pu-239	2.62×10^{0}
Ta-182	1.87×10^{10}	Ta-182	2.05×10^{0}
Co-58	1.78×10^{10}	Xe-133	1.81×10^{0}
Fe-55	1.65×10^{10}	Pu-238	1.01×10^{0}
		Pu-241	5.72×10^{-1}
	30 days		
Sc-46	4.77×10^{11}	Sc-46	5.75×10^{1}
Ca-45	3.26×10^{11}	Ca-45	2.14×10^{1}
Fe-55	1.62×10^{10}	Co-60	7.94×10^{0}
Ta-182	1.57×10^{10}	Pu-239	4.26×10^{0}
Co-60	1.45×10^{10}	Ta-182	2.78×10^{0}
Co-57	1.34×10^{10}	Pu-238	1.64×10^{0}
Co-58	1.34×10^{10}	Pu-241	9.21×10^{-1}
W-185	3.32×10^{9}	Pu-240	5.77×10^{-1}
		Co-58	4.98×10^{-1}
	1 year		
Ca-45	7.85×10^{10}	Co-60	2.81×10^{1}
Sc-46	2.99×10^{10}	Ca-45	2.06×10^{1}
Fe-55	1.28×10^{10}	Pu-239	1.70×10^{1}
Co-60	1.28×10^{10}	Sc-46	1.44×10^{1}
Co-57	5.70×10^{9}	Pu-238	6.52×10^{0}
Ta-182	2.07×10^{9}	Pu-241	3.52×10^{0}
Mn-54	1.42×10^{9}	Pu-240	2.30×10^{0}
Ag-110m	7.37×10^{8}	Kr-85	1.55×10^{0}
		Ta-182	1.46×10^{0}
		Ar-39	9.64×10^{-1}
		Fe-55	7.00×10^{-1}
		Ag-110m	6.26×10^{-1}
		Am-241	5.58×10^{-1}

Table 14. *Cont.*

Isotope	Activity, Bq/kg	Isotope	Dose Rate Inhalation, %
		10 years	
Co-60	3.92×10^{9}	Pu-239	4.15×10^{1}
Fe-55	1.31×10^{9}	Co-60	2.10×10^{1}
Ni-63	9.93×10^{7}	Pu-238	1.48×10^{1}
C-14	1.78×10^{7}	Pu-240	5.62×10^{0}
		Pu-241	5.56×10^{0}
		Am-241	5.50×10^{0}
		Ar-39	2.30×10^{0}
		Kr-85	2.12×10^{0}
		Ar-42	9.99×10^{-1}
		Fe-55	1.75×10^{-1}
		100 years	
Ni-63	5.34×10^{7}	Pu-239	6.09×10^{1}
C-14	1.76×10^{7}	Am-241	1.70×10^{1}
Ag-108m	3.17×10^{6}	Pu-238	1.07×10^{1}
Pu-239	2.00×10^{6}	Pu-240	8.19×10^{0}
U-235m	2.00×10^{6}	Ar-39	2.68×10^{0}
Cs-137	1.15×10^{6}	Ar-42	2.22×10^{-1}
Ba-137m	1.09×10^{6}		
Ni-59	7.88×10^{5}		
Am-241	6.96×10^{5}		
Y-90	4.89×10^{5}		
Sr-90	4.89×10^{5}		
Be-10	4.81×10^{5}		

5. Recycling Possibilities for the Irradiated $Be_{12}Ti$

For the DEMO fusion reactor, the two operation phases are considered with durations of 5.2 and 14.8 calendar years. Because of the limited world Be resources, a recycling option should also be considered to relax or decrease the Be demands for the HCPB DEMO blankets in the second phase. Any recycling strategy has to include the following three generic steps: (1) detritiation, (2) purification or removal of the radioactive products and (3) production of the $Be_{12}Ti$ blocks.

The basic procedure for the tritium removal from the irradiated $Be_{12}Ti$ blocks is high-temperature annealing. The experiments performed at the irradiated Be samples show that tritium release has a non-diffusive (explosive) nature [10]: the tritium release reaction rate as a function of the annealing temperature has a sharp peak. The effective temperature of the peak depends on the neutron fluence applied to the samples: the higher the fluence, the more the tritium atoms accumulate and the lower the peak of the annealing temperature. The sample heating rate also affects the peak temperature: the increase in the rate leads to the decrease in the peak temperature [10]. We expect that the detritiation of the $Be_{12}Ti$ blocks follows the same tendencies. The temperature of the peaks for an efficient tritium release varies from ~400 to 900 °C depending on the irradiation history and the heating rate. The peak value of the tritium concentration in the irradiated $Be_{12}Ti$ calculated in the equatorial mid plane of the blanket was assessed without implementation of the tritium removal rate and it was estimated to be ~$1.9 \cdot 10^{12}$ Bq/g right after the reactor shutdown. This value drastically exceeds the clearance limit of 100 Bq/g [11]. It exceeds by ~10,000 times and ~2000 times the limits accepted in the Centre Stockage de l'Aube and in the El Cabril facilities, respectively (Tables 8 and 9). Therefore, the deep and long detritiation procedure seems to be absolutely necessary to assure the safe treatment of the

irradiated $Be_{12}Ti$. The duration of the annealing procedure to reach the acceptable level of the tritium concentration is beyond the subject of this paper.

In the case of the full recycling of the irradiated $Be_{12}Ti$, the purification process should follow the detritiation of the blocks. Nowadays, the technology for the recycling of the irradiated Be and, moreover, for the irradiated $Be_{12}Ti$, does not exist in an industrial scale. The attempts for purification of the normal metallic Be were already performed making use of different technologies: vacuum distillation, zone melting and chlorine processes [37]. The chlorine method includes the chlorination of beryllium and then the reduction of the beryllium chloride to pure metallic Be. Beryllium halides are fairly volatile at high temperatures (up to 1500 °C) and they are much more volatile compared to the impurities in halides. This route is used to obtain high-purity beryllium. The degree of the purification depends on a number of cycles applied: dissolution, precipitation and washing. The decontamination factor could vary from ~$10^2 \div 10^4$ and be higher depending on the cycle number ($1 \div 3$) and the duration of the whole procedure could take up to 1 year [38]. The final product very likely will still contain some residual radioactivity preventing its conventional treatment without clearance. This refining process is very energy consuming and additionally it requires a significant amount of the dangerous acid. Overall, this procedure is harmful and in general, environmentally unfriendly. To avoid the additional environmental burden, a special purification factory should be constructed close to the DEMO site. This factory should be naturally protected against any radioactive leakage to the environment. It should also be fully automated and the remote handling has to be widely implemented. Applied to the irradiated $Be_{12}Ti$, the purification process seems to be very expensive resulting in a significant price increase for the final product. Whether the purification of the irradiated $Be_{12}Ti$ is worth developing for the DEMO materials' recycling is beyond the scope of this work.

The last step in the theoretical recycling route of the irradiated $Be_{12}Ti$ is a refabrication of the blocks. If the purified $Be_{12}Ti$ is available as in the result of the previous step, the manufacturing of the new blocks follows the already well-established technology from the fresh Be and Ti. After the purification process, remote handling would be necessary to exclude the personnel radiation exposure. Because of the residual activity, the remote handling for the manufacture of the new blocks and blankets afterwards looks to be unavoidable. The purification step could be fully skipped. In this case, after the detritiation, the irradiated $Be_{12}Ti$ blocks would be directed to the refabricating facility. The secure and well-protected facility against operational and environmental contamination seems to be conceivable or even theoretically feasible. Such a plant has to include a pressing machine for the crushing of the $Be_{12}Ti$ blocks and another one for the refabricating of the blocks. The remote control and handling are therefore necessary for the final blanket fabrication. This theoretical option could only be feasible if the irradiated $Be_{12}Ti$ is allowed to be used for the HCPB blanket fabrication and the proper technology is developed, approved and certified for the secure application.

6. Conclusions

The activity and the disposal options of the irradiated $Be_{12}Ti$ were assessed for the HCPB DEMO blankets making use of a code system that enables performing 3D activation calculations by linking the Monte Carlo transport code MCNP and the fusion inventory code FISPACT through the appropriate interface. The dedicated full-scale geometry MCNP model of the 11.25 degree HCPB DEMO torus was adapted to the requirements for the coupled 3D neutron transport and activation calculations. Special attention was paid to the use in the activation calculations of the commercial materials containing technological impurities. This has a crucial effect on the results and the impurities must be carefully accounted for in any nuclear safety analyses.

The activation analyses were performed for the HCPB DEMO breeder blankets for several decay cooling times from shutdown up to 100 years. The method used enabled the calculations for the activity of the $Be_{12}Ti$ in different locations in the HCPB blankets.

The total activity of the $Be_{12}Ti$ ("average" material composition) in the whole reactor is ~$5.42 \cdot 10^{17}$ Bq right after the reactor shutdown and it decreases up to ~$7.2 \cdot 10^{15}$ Bq after 1 month. For the longer cooling time, the differences in the total activity of the $Be_{12}Ti$ with various material compositions become more significant and the activity has the deviation for different material compositions. The short-term activity is formed by the radionuclides produced through the activation of Be and Ti nuclei and the long-term activity is formed by the products of the neutron irradiation taking place on the impurities.

A prerequisite for the disposal or the recycling of the irradiated $Be_{12}Ti$ is its deep detritiation; otherwise, the very high-tritium activity would fully prevent any attempt for its treatment. The most preferable is the use of the $Be_{12}Ti$ from the Ulba factory: this material composition includes fewer material impurities, especially uranium. The uranium impurity should be kept at the level below 0.002 wt.% to satisfy the safety limits for the storage. The disposal of the $Be_{12}Ti$ blocks irradiated in the HCPB DEMO is not possible 100 years after the reactor shutdown in the UK repositories. There could be the option to dispose the $Be_{12}Ti$ intermediate-level wastes in the French repository after 1 year of cooling assuming the detailed control of the impurities that fulfil the French authority requirements. The fission products resulting from the uranium impurity do not represent the environmental risk, for both short- and long-term disposal strategies of the irradiated $Be_{12}Ti$. The El Cabril repository could also be the proper site for the disposal of the irradiated $Be_{12}Ti$ if the integral limits will not be applied in this case. The German repository even in spite of its large capacity does not provide enough space for the $Be_{12}Ti$ wastes' storage. In the case of the theoretical possibility for the $Be_{12}Ti$ disposal, the safety limits applied in Germany prevent its storage in the repositories. The USA near-ground repositories could be an alternative to the European sites. The tritium retention in the irradiated $Be_{12}Ti$ has to be well investigated and assessed to control the tritium activity and to develop the disposal strategy to ensure secure disposal options. The $Be_{12}Ti$ blocks irradiated in the HCPB DEMO blankets could be securely disposed in several repositories worldwide (for instance, in France or in the USA) in case of the use of the Be ore with low-uranium impurity (for example, Ulba beryllium resources).

The well-elaborated and certified recycling option of the irradiated $Be_{12}Ti$ blocks is not yet addressed and developed. The remote handling technology for the re-fabrication of the blocks from the irradiated material has to be well tested, approved and certified. The location for the manufacturing facility should be close to the reactor site to avoid the transportation of the activated materials over well-populated regions. Such a procedure will significantly increase the capital DEMO costs and probably result in a public rejection of the whole project. In light of these heavy conditions, the recycling of the activated $Be_{12}Ti$ seems to be questionable and it requires significant investigations of its practical feasibility.

Author Contributions: Conceptualization, P.P., P.C. and J.E.-U.; methodology, P.P.; software, P.P.; validation, P.P., P.C. and J.E.-U.; formal analysis, P.P.; investigation, P.P.; resources, P.C. and J.E.-U.; data curation, P.C. and J.E.-U.; writing—original draft preparation, P.P.; writing—review and editing, P.C. and J.E.-U.; visualization, P.P.; supervision, P.C.; project administration, P.C. and J.E.-U.; funding acquisition, J.E.-U. All authors have read and agreed to the published version of the manuscript.

Funding: This work has been carried out within the framework of the EUROfusion Consortium, funded by the European Union via the Euratom Research and Training Programme (Grant Agreement No 101052200—EUROfusion). Views and opinions expressed are, however, those of the author(s) only and do not necessarily reflect those of the European Union or the European Commission. Neither the European Union nor the European Commission can be held responsible for them.

Institutional Review Board Statement: Not applicable.

Informed Consent Statement: Not applicable.

Data Availability Statement: Data is unavailable due to privacy restrictions.

Conflicts of Interest: The authors declare no conflict of interest.

References

1. Federici, G. Maturation of critical technologies and systems design. *Fusion Eng. Des.* **2022**, *177*, 113082. [CrossRef]
2. Arena, P.; Del Nevo, A.; Moro, F.; Noce, S.; Mozzillo, R.; Imbriani, V.; Giannetti, F.; Edemetti, F.; Froio, A.; Savoldi, L.; et al. The DEMO Water-Cooled Lead–Lithium Breeding Blanket: Design Status at the End of the Pre-Conceptual Design Phase. *Appl. Sci.* **2021**, *11*, 11592. [CrossRef]
3. Hernández, F.A.; Pereslavtsev, P.; Zhou, G.; Kang, Q.; D'amico, S.; Neuberger, H.; Boccaccini, L.V.; Kiss, B.; Nádasi, G.; Maqueda, L.; et al. Consolidated design of the HCPB Breeding Blanket for the pre-Conceptual Design Phase of the EU DEMO and harmonization with the ITER HCPB TBM program. *Fusion Eng. Des.* **2020**, *157*, 111614. [CrossRef]
4. Kelly, T.D.; Matos, G.R. U.S. Geological Survey, Beryllium statistics. Historical statistics for mineral and material commodities in the United States. U.S. Geological Survey Data Series 140. 2014. Available online: https://www.usgs.gov/centers/national-minerals-information-center/historical-statistics-mineral-and-material-commodities#bariteandhttps://www.usgs.gov/media/files/beryllium-historical-statistics-data-series-140 (accessed on 18 June 2023).
5. U.S. Geological Survey. *Mineral Commodity Summaries 2022*; U.S. Geological Survey: Washington, DC, USA, 2022; 202p. [CrossRef]
6. Park, J.H.; Pereslavtsev, P. Comparative activation analyses for the HCPB breeding blanket in DEMO. *Fusion Eng. Des.* **2021**, *167*, 112338. [CrossRef]
7. Foley, N.K.; Jaskula, B.W.; Piatak, N.M.; Schulte, R.F. *Critical Mineral Resources of the United States—Economic and Environmental Geology and Prospects for Future Supply*; Schulz, K.J., DeYoung, J.H., Jr., Seal, R.R., II, Bradley, D.C., Eds.; U.S. Geological Survey Professional Paper 1802; USGS: Washington, DC, USA, 2017; pp. E1–E32. [CrossRef]
8. Gaisin, R.; Chakin, V.; Vladimirov, P.; Hernández, F.A.; Udartsev, S.; Vechkutov, A.; Kolmakov, M. Industrial-scale manufacturing experience of titanium beryllide block for DEMO blanket application. *Fusion Eng. Des.* **2020**, *161*, 111862. [CrossRef]
9. Available online: https://materion.com/products/beryllium-products/beryllium-metal (accessed on 18 June 2023).
10. Kolbasov, B.; Khripunov, V.; Biryukov, A. On use of beryllium in fusion reactors: Resources, impurities and necessity of detritiation after irradiation. *Fusion Eng. Des.* **2016**, *109–111*, 480–484. [CrossRef]
11. International Atomic Energy Agency. *Application of the Concepts of Exclusion, Exemption and Clearance: Safety Guide*; Safety Standards Series; International Atomic Energy Agency: Vienna, Austria, 2004; p. 24. ISSN 1020-525X. no. RS-G-1.7. STI/PUB/1202; ISBN 92-0-109404-3.
12. Gliss, C.; Ciattaglia, S.; Korn, W.; Moscato, I. Initial layout of DEMO buildings and configuration of the main plant systems. *Fusion Eng. Des.* **2018**, *136 Pt A*, 534–539. [CrossRef]
13. Armstrong, J.C.; Brown, F.B.; Bull, J.S.; Casswell, L.; Cox, L.J.; Dixon, D.; Forster, R.A.; Goorley, J.T.; Hughes, H.G.; Favorite, J.; et al. *MCNP User's Manual Code Version 6.2.*; Werner, C.J., Ed.; Los Alamos National Laboratory Tech. Rep. LA-UR-17-29981; MCNP: Los Alamos, NM, USA, 2017.
14. Fleming, M.; Stainer, T.; Gilbert, M. *The FISPACT II User Manual*; UKAEA-R(18)001; UK Atomic Energy Authority, Culham Science Center: Abingdon, UK, 2018.
15. Plompen, A.J.M.; Cabellos, O.; Jean, C.D.S.; Fleming, M.; Algora, A.; Angelone, M.; Archier, P.; Bauge, E.; Bersillon, O.; Blokhin, A.; et al. The joint evaluated fission and fusion nuclear data library, JEFF-3.3. *Eur. Phys. J. A* **2020**, *56*, 181. [CrossRef]
16. Koning, A.; Rochman, D.; Sublet, J.-C.; Dzysiuk, N.; Fleming, M.; van der Marck, S. TENDL: Complete Nuclear Data Library for Innovative Nuclear Science and Technology. *Nucl. Data Sheets* **2019**, *155*, 1–55. [CrossRef]
17. Eade, T.; Garcia, M.; Garcia, R.; Ogando, F.; Pereslavtsev, P.; Sanz, J.; Stankunas, G.; Travleev, A. Activation and decay heat analysis of the European DEMO blanket concepts. *Fusion Eng. Des.* **2017**, *124*, 1241–1245. [CrossRef]
18. Chakin, V.; Rolli, R.; Gaisin, R.; Hoeppener-Kramar, U.; Nakamichi, M.; Zmitko, M. Tritium release and retention in beryllium and titanium beryllide after neutron irradiation up to damage doses of 23-38 dpa. *Fusion Eng. Des.* **2020**, *161*, 111938. [CrossRef]
19. International Atomic Energy Agency. *Classification of Radioactive Waste*; IAEA Safety Standards Series No. GSG-1; IAEA: Vienna, Austria, 2009.
20. De Vicente, S.M.G.; Smith, N.A.; El-Guebaly, L.; Ciattaglia, S.; Di Pace, L.; Gilbert, M.; Mandoki, R.; Rosanvallon, S.; Someya, Y.; Tobita, K.; et al. Overview on the management of radioactive waste from fusion facilities: ITER, demonstration machines and power plants. *Nucl. Fusion* **2022**, *62*, 085001. [CrossRef]
21. Bergström, U.; Pers, K.; Almén, Y. *International Perspective on Repositories for Low Level Waste*; SKB R-11-16; SKB International AB: Stockholm, Sweden, 2011; ISSN 1402-3091.
22. Gilbert, M.R.; Eade, T.; Rey, T.; Vale, R.; Bachmann, C.; Fischer, U.; Taylor, N. Waste implications from minor impurities in European DEMO materials. *Nucl. Fusion* **2019**, *59*, 076015. [CrossRef]
23. UK Department of Energy & Climate Change. Strategy for the Management of Solid Low Level Radioactive Waste from the Non-Nuclear Industry in the United Kingdom, 2016. Available online: https://assets.publishing.service.gov.uk/government/uploads/system/uploads/attachment_data/file/497114/NI_LLW_Strategy_Final.pdf, (accessed on 18 June 2023).
24. Morales, A. Characterization and acceptance criteria of conditioned radioactive wastes at El Cabril disposal facility. *Nucl. Eng. Des.* **1997**, *176*, 177–180. [CrossRef]
25. Morales, A. El Cabril low and intermediate level waste disposal facility (Spain): New acceptance criteria. In Proceedings of the Waste Management Symposium 2005, Tucson, AZ, USA, 27 February–3 March 2005. Available online: https://archivedproceedings.econference.io/wmsym/pdfs/5035.pdf (accessed on 18 June 2023).

26. Kekki, T.; Tiitta, A. *Evaluation of the Radioactive Waste Characterisation at the Olkiluoto Nuclear Power Plant*; STUK-YTO-TR162; VTT Chemical Technology: Helsinki, Finland, 2000.
27. Cox, B. *Basis for National and International Low Activity and Very Low Level Waste Disposal Classifications*; EPRI: Palo Alto, CA, USA, 2012; p. 1024844.
28. Gagner, L.; Voini, S. Derivation of waste acceptance criteria for low intermediate level waste in surface disposal facility, activity limits at the Centre de l'Aube. In Proceedings of the International Conference on Nuclear Option in Countries with Small and Medium Electricity Grids, Dubrovnik, Croatia, 19–22 June 2000; p. 780.
29. Upstream Optioneering ILW/LLW Opportunities: Identification of Potential Opportunities for ILW/LLW Boundary Wastes Introduced by Changing Disposal Route, June 2014, AMEC, 201139-AA-0004/001/Issue 1. Available online: https://webarchive.nationalarchives.gov.uk/ukgwa/20211004151355/https://rwm.nda.gov.uk/publication/upstream-optioneering-llw-ilw-opportunities-identification-of-potential-opportunities-for-ilw-llw-boundary-wastes-introduced-by-changing-disposal-route/?download (accessed on 18 June 2023).
30. Agence Nationale pour la Gestion des Déchets Radioactifs (Andra), Centre de Stockage de l'Aube (CSA)—INB n°149, Demande de Modification Portant sur la Prise en Charge de Colis de Sources Scellées Usagées de Forte Activité, Lettre ASN CODEP-CHA-2018-023387 du 13 Juin 2018, Institut de Radioprotection et de Surete Nucleaire (IRSN). Available online: https://www.irsn.fr/sites/default/files/documents/expertise/avis/2019/Avis-IRSN-2019-00179.pdf (accessed on 18 June 2023).
31. ANDRA. National Radioactive Waste Management Agency. In *ACO.SP.ASRE.99.001D and ACO.SP.ASRE.99.0002D ANDRA Specifications*; ANDRA: Châtenay-Malabry, France, 2014.
32. Zucchetti, M.; Di Pace, L.; El-Guebaly, L.; Kolbasov, B.; Massaut, V.; Pampin, R.; Wilson, P. An integrated approach to the back-end of the fusion materials cycle. *Fusion Eng. Des.* **2009**, *52*, 109–139. [CrossRef]
33. NEA; OECD. *Preservation of Records. Knowledge and Memory (RK&M) across Generations: Compiling a Set of Essential Records for a Radioactive Waste Repository*; Nuclear Energy Agency (NEA); OECD: Paris, France, 2019; No. 7423.
34. Daniels, N.; Deissmann, G.; Modolo, G.; Bosbach, D. *Fachlicher Abschlussbericht des BMBF geförderten Verbundvorhabens: "Konzeptstudie zur Entsorgung von Aktiviertem Beryllium aus Forschungsreaktoren (KONEKT)"*; Förderkennzeichen 15S9405A-B; Federal Ministry of Education and Research: Bonn, Germany, 2021.
35. Brennecke, P. *Requirements on Radioactive Waste for Disposal (Waste Acceptance Requirements as of December 2014)*; Konrad Repository; SE-IB-29/08-REV-2; BfS—Federal Office for Radiation Protection: Salzgitter, Germany, 2015.
36. United States Nuclear Regulatory Commission. Waste Classification §61.55, Part 61—Licensing Requirements for Land Disposal of Radioactive Waste. NRC Regulations Title 10, Code of Federal Regulations. Available online: https://www.nrc.gov/reading-rm/doc-collections/cfr/part061/part061-0055.html (accessed on 18 June 2023).
37. Druyts, F.; Dylst, K.; Braet, J. Beryllium recycling: Feasibility and challenges. In Proceedings of the 8th IEA International Workshop on Beryllium Technology, Lisbon, Portugal, 5–7 December 2007.
38. Posevin, A.O.; Levakov, B.I.; Demchenko, N.F.; Pokrovskii, A.S.; Belozerova, A.R. Decontamination of irradiated beryllium from radioactive impurities by precipitation of hydroxides in the presence of a complexone. *Radiochemistry* **2015**, *57*, 92–97. [CrossRef]